

On-Wafer Noise-Parameter Measurement Using Wide-Band Frequency-Variation Method

Robert Hu and Tzu-Hsien Sang

Abstract—In this paper, it is demonstrated that the newly proposed wide-band frequency-variation method, where only one set of matched and mismatched noise measurements is used, can efficiently determine the noise parameters of an ultra-sensitive transistor on-wafer at room temperature. Since the experimental setup is similar to that of conventional noise-temperature measurement while no complicated hardware is employed, this new approach is straightforward, yet efficient, and can be easily extended to applications with much higher or broader frequency ranges. Both the measured noise parameters of the post-amplifier stage and the transistor under test will be presented and investigated.

Index Terms—Frequency variation, noise parameters.

I. INTRODUCTION

RECENTLY, we proposed a novel wide-band frequency-variation method for the purpose of measuring the cryogenic noise parameters of a wide-band low-noise amplifier (LNA), and it is revealed that this method works equally well at room temperature for both passive circuits and LNAs [1]. In this paper, a wide-band frequency-variation method is adopted in measuring the noise parameters of an ultra-sensitive transistor on-wafer at room temperature. Since neither prerequisite noise model of the transistor, nor any complicated tuner technique is required [2], [3], this approach is reliable and convenient.

One challenge in measuring the noise parameters of an ultra-sensitive transistor is, in addition to its low noise temperature, that for certain generator reflection coefficient (Γ_g), the transistor's output reflection coefficient can be larger than one and, thus, cause system instability. While it is true in the tuner case that if a chosen Γ_g brings in oscillation, it can be deemed unsuitable and soon be replaced by another tuner setting; in the wide-band frequency-variation method, on the contrary, once the implemented Γ_g causes instability, the only choice is to revise the whole system. In other words, the conditional stability of the transistor itself not only imposes a restriction on the available Γ_g , but also demands a well-performing post-amplifier.

In this paper, the experimental setup and its design methodology will be discussed first. Measured noise parameters of the post-amplifier, where the resistive-feedback circuit configuration is used, are then presented. The reason why this amplifier is nearly matched in terms of noise will be addressed as well. As for the transistor, a revised algorithm for the noise parameter calculation is proposed that is then followed by the measured noise

Manuscript received September 28, 2004; revised December 12, 2004. This work was supported in part by the National Aeronautics and Space Administration under Grant NAG5-9493 and by the National Science Council of Taiwan under Contract NSC 93-2218-E-009-068.

The authors are with the Department of Electronics Engineering, National Chiao-Tung University, Taiwan, R.O.C.

Digital Object Identifier 10.1109/TMTT.2005.850425

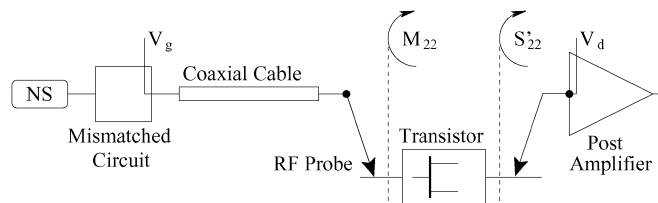


Fig. 1. On-wafer noise-parameter measurement setup using wide-band frequency-variation method.

parameters to demonstrate the feasibility of this new noise measurement approach.

II. EXPERIMENTAL SETUP

The noise temperature T_n of a two-port circuit can be expressed as a function of four noise parameters T_{\min} , N , Γ_{opt} ($= \gamma_{\text{opt}} \exp(j\theta_{\text{opt}})$)

$$T_n = T_{\min} + 4T_0N \frac{|\Gamma_g - \Gamma_{\text{opt}}|^2}{(1 - |\Gamma_g|^2)(1 - |\Gamma_{\text{opt}}|^2)} \quad (1)$$

where T_{\min} is the minimum noise temperature, N is the noise ratio, Γ_{opt} is the optimum reflection coefficient, Γ_g is the generator reflection coefficient, and T_0 is simply 290 K. Recently, we demonstrated that one set of matched and mismatched noise-temperature measurements is mathematically sufficient in deriving the four unknown noise parameters over a wide frequency range, known as the wide-band frequency-variation method.

In measuring the noise parameters of the transistor using the wide-band frequency-variation method, the experimental setup is similar to that of the 50- Ω noise-temperature measurement. As illustrated in Fig. 1, in the mismatched noise-temperature measurement, the mismatched circuit and coaxial cable will cause the noise temperature of the transistor versus frequency to be highly periodic; while in the matched case, the mismatched circuit is replaced by a matched bias-tee for the transistor's gate bias. Here, the noise source (NS) is Agilent N4000A. The output of the custom-made post-amplifier is connected to the Agilent noise-figure analyzer.

Fig. 2 shows the mismatched and matched generator reflection coefficients, which are measured with reference to the input of the transistor. The rapid clockwise phase variation as frequency increases is due to the combined effect of the coaxial cable and the RF probe in front of the transistor. Details of the mismatched circuit can be found in [1]. The nonzero generator reflection coefficient in the matched case is due to the finite output reflection coefficients of the NS and the bias-tee. Due to the finite isolation of the transistor under test, the measured output reflection coefficient (in decibels) of the transistor in

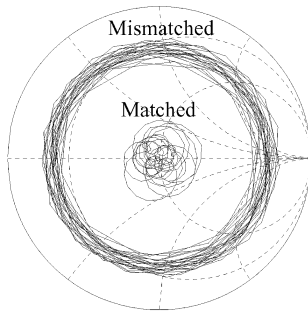


Fig. 2. 3–18-GHz matched and mismatched generator reflection coefficients, i.e., M_{22} of Fig. 1.

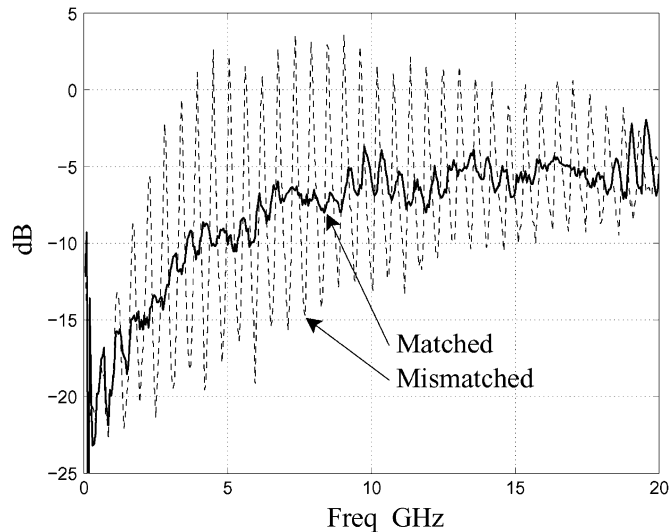


Fig. 3. Measured output reflection coefficient of the transistor, i.e., S'_{22} of Fig. 1, in the matched and mismatched cases.

the mismatched case can be positive at several frequencies, as displayed in Fig. 3. In the matched case (solid curve), the measured curve is below 0 dB; while in the mismatched case (dashed curve), it can be positive and make the system unstable if the post-amplifier does not have a matched input over the whole bandwidth. The diminishing magnitude of the mismatched curve for frequencies below 5 GHz is due to the low reflection coefficient of the mismatched circuit at these frequencies; otherwise, the large ripples at the low end of the frequency will render this system useless, as can be easily noticed from the bias oscillation of the post amplifier. Therefore, to ensure the system stability, a resistive-feedback amplifier is designed to have a low input reflection coefficient over a wide bandwidth. The use of isolator is ruled out because of its limited bandwidth, and so is the balanced configuration.

By directly connecting to the RF probe, this post-amplifier not only contributes less noise temperature, but also has its noise parameters less frequency dependent than if a coaxial cable is inserted between this amplifier and the RF probe. The amplifier's 40-mW power dissipation is low and will not heat up the transistor on-wafer, as otherwise can be observed from the rising with time of the measured noise temperature. Commercial amplifiers, such as the MITEQ-AFS4 series LNAs that dissipate hundreds of milliwatts, are not suitable here for two reasons. First, even if a large heat sink can be attached to this amplifier

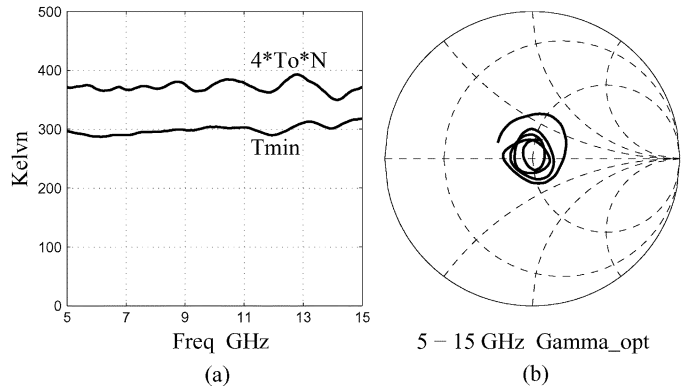


Fig. 4. 5–15-GHz measured noise parameters of the post-amplifier stage. (a) T_{\min} and $4T_0N$. (b) Γ_{opt} .

to effectively reduce the temperature of the chassis, the heat generated inside can still flow through its input connector's central metal pin to the RF probe, and then to the transistor under test. Second, if a long coaxial cable is inserted as a thermal buffer between this amplifier and RF probe, noise parameters of the post-amplifier stage where the cable is included will change at a rate comparable to or even larger than that of Γ_g in the mismatched noise measurement, which implies the measured noise parameters of the post-amplifier stage cannot be accurate.

As for the RF probe, its S -parameters also need to be known to correctly account for its noise impact [4]. For the GGB 40A-GSG-100P probe, it has $S_{21} = 0.965$, i.e., -0.3 dB, at 10 GHz, which will contribute a matched noise temperature of 21 K and is quite comparable to that of the transistor under test. The measured S_{11} are all below -25 dB. Knowing the S -parameters of the RF probe and other related passive circuits, the measured overall noise temperatures can then be properly deembedded; noise parameters of the post-amplifier stage are, therefore, derived from the corresponding matched and mismatched data.

III. NOISE PARAMETERS OF THE POST-AMPLIFIER STAGE

As the post-amplifier's noise temperature is strongly influenced by its 400- Ω feedback resistor, the measured T_{\min} , N and $|\Gamma_{\text{opt}}|$ of the post-amplifier stage tend to be independent of frequency, while the large phase variation of the measured Γ_{opt} versus frequency is mainly due to its input RF probe, as shown in Fig. 4, which includes the RF probe and its following post-amplifier. In Fig. 4(a), both the minimum noise temperature T_{\min} and the product $4T_0N$ have units of kelvins. Fig. 4(b) shows the optimum reflection coefficient Γ_{opt} that moves counterclockwise as frequency increases. The large phase variation of Γ_{opt} is mainly due to the physical dimension of the RF probe.

A quick inspection on the value of $4T_0N/T_{\min}$, which lies between 1 and 2, suggests that the derived noise parameters are reasonable [5]. Using the definition of noise temperature, the matched and mismatched noise temperatures can, in turn, be reconstructed from the just derived noise parameters. Both agree well with the raw data, as shown in Fig. 5. Here, Fig. 5(a) corresponds to the matched case, where the solid curve is the measured noise temperature, while the dashed curve is its simulated counterpart, which is based on the just-derived noise parameters. Fig. 5(b) shows the measured (solid curve) and simulated

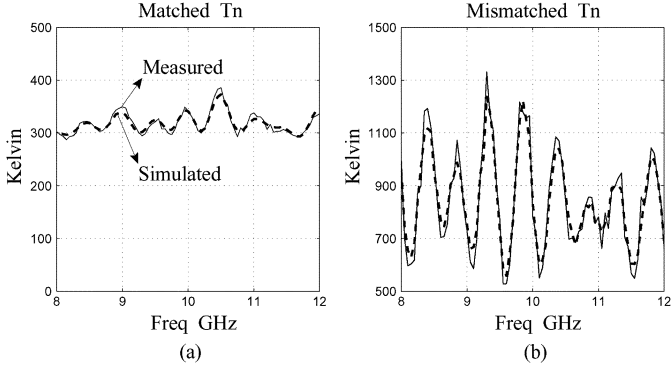


Fig. 5. 8–12-GHz matched and mismatched noise temperatures of the post-amplifier stage. (a) Matched T_n . (b) Mismatched T_n .

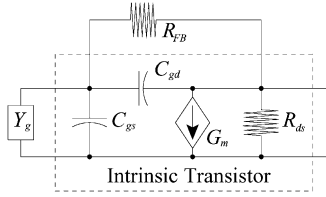


Fig. 6. Resistive-feedback circuit configuration used for explaining the nearly matched noise temperature of the post-amplifier.

(dashed curve) noise temperatures in the mismatched case. In both graphs, it is 8–12 rather than 5–15 GHz on the X -axis for the purpose of clearer comparison between the measured and simulated curves.

The reason why this resistive-feedback post-amplifier has an almost-matched Γ_{opt} , which implies that the matched T_n is close to T_{min} , is intriguing. Of course, if most of the noise comes from the output part of the circuit, then Γ_{opt} will follow the conjugate of the input reflection coefficient, and then results in a matched Γ_{opt} . However, this is too bold an assumption since the feedback (parallel) resistor will contribute noise to both the transistor's gate and drain ports, and, unlike the case where a shunt resistor is directly added to the input of the circuit, the noise generated at the input part of the circuit cannot be treated as uncorrelated to the noise coming from the output part of the circuit. An explicit noise-temperature derivation is, therefore, necessary. In Fig. 6, the temperature of the feedback resistor R_{FB} is set to be the ambient temperature T_{amb} ; that of the intrinsic resistor R_{ds} is an artificial temperature T_{drain} . The intrinsic gate resistor R_{gs} , which is only a few ohms, is omitted here to simplify the noise derivation.

First, since the noise wave from the feedback resistor $R_{\text{FB}} (=1/G_{\text{FB}})$ itself is indeed not correlated to the noise wave from the transistor's intrinsic resistor R_{ds} , the noise temperature of this circuit will be

$$\begin{aligned}
 T_n = & \frac{T_{\text{amb}}}{G_m^2} \frac{1}{R_{\text{FB}} G_g} (G_g + 2G_{\text{FB}} + G_m)^2 \\
 & + \frac{T_{\text{amb}}}{G_m^2} \frac{1}{R_{\text{FB}} G_g} (B_g + \omega C_{\text{gs}} + \omega C_{\text{gd}})^2 \\
 & + \frac{T_{\text{drain}}}{G_m^2} \frac{1}{R_{\text{ds}} G_g} (G_g + G_{\text{FB}})^2 \\
 & + \frac{T_{\text{drain}}}{G_m^2} \frac{1}{R_{\text{ds}} G_g} + (B_g + \omega C_{\text{gs}} + \omega C_{\text{gd}})^2. \quad (2)
 \end{aligned}$$

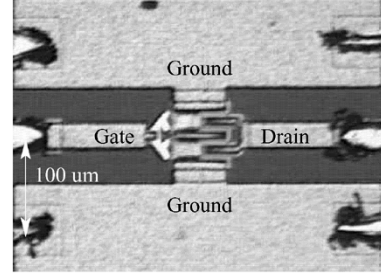


Fig. 7. High electron-mobility transistor under test.

By setting the imaginary part of the generator admittance $Y_g (=G_g + jB_g)$ as

$$B_{\text{opt}} = -\omega(C_{\text{gs}} + C_{\text{gd}}) \quad (3)$$

which is a small number, the capacitor-related terms in the above T_n expression can be removed. By letting $\alpha = (R_{\text{ds}}/R_{\text{FB}})(T_{\text{amb}}/T_{\text{drain}})$, the value of G_g that corresponds to the minimum noise temperature is

$$G_{\text{opt}} = G_{\text{FB}} \sqrt{\frac{1 + \alpha(G_m/G_{\text{FB}})^2}{1 + \alpha}} \approx G_m \sqrt{\frac{R_{\text{ds}} T_{\text{amb}}}{R_{\text{FB}} T_{\text{drain}}}}. \quad (4)$$

For $T_{\text{drain}} = 2500$ K, $T_{\text{amb}} = 300$ K, $R_{\text{FB}} = 400 \Omega$, $R_{\text{ds}} = 100 \Omega$, and $G_m = 120$ mS, there is $1/G_{\text{opt}} = 48 \Omega$, i.e., an almost-matched optimum reflection coefficient. One implication of the above derivations is that, if a transistor circuit with feedback resistor is designed to have low input reflection coefficient and good noise match at room temperature, a cryogenically signal-matched input, as mainly determined by G_m , R_{ds} , and R_{FB} , cannot guarantee an accompanying noise match unless T_{amb} and T_{drain} vary proportionally to each other.

IV. NOISE PARAMETERS OF THE TRANSISTOR

Once the noise parameters of the post-amplifier stage are known, matched and mismatched noise temperatures of the transistor, which is a high electron-mobility transistor, can be properly deembedded. In this transistor (Fig. 7), the gate on the left-hand side is split into four 50- μm -long branches and, thus, has a total length of 200 μm , which is more than the 150 μm used in the post-amplifier. The drain bias voltage and current are $V_d = 0.6$ V and $I_d = 12$ mA, with gate voltage set to -0.19 V and gate current in the microampere range. Though this ultra-sensitive transistor, as fabricated by Northrop Grumman Space Technology (NGST), Redondo Beach, CA, using 0.1- μm InP technology has long been employed in the design of wide-band LNAs for radio-astronomical applications [6], [7], its noise characteristics have not been fully explored.

In extracting the four noise parameters, noise temperature expression needs to be linearized before applying the least squares fit, as was explained in Section II. To reduce the impact of measurement errors, two-step linearization is usually the preferred approach [8]. First, the value of θ_{opt} can be obtained from the phase of the measured mismatched noise temperature via high-precision sinusoid estimation methods [9], [10]; with this

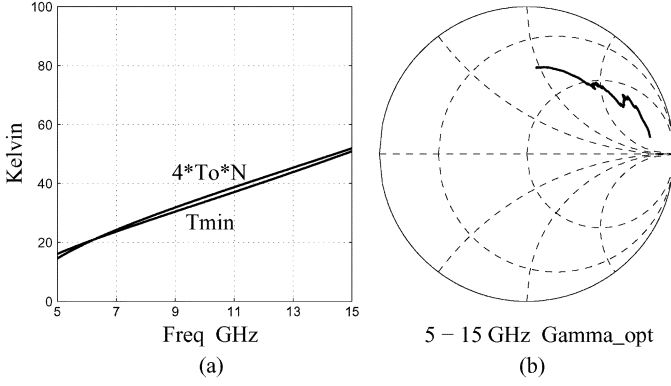


Fig. 8. 5–15-GHz measured noise parameters of the transistor. (a) T_{\min} and $4T_0N$. (b) Γ_{opt} .

known θ_{opt} , noise temperature can now be linearized in terms of three, instead of four, new variables a, b, c

$$\begin{aligned} a &= -4T_0N \frac{1}{1 - \gamma_{\text{opt}}^2} + T_{\min} \\ b &= 4T_0N \frac{1 + \gamma_{\text{opt}}^2}{1 - \gamma_{\text{opt}}^2} \\ c &= -8T_0N \frac{\gamma_{\text{opt}} \cos(\theta_{\text{opt}})}{1 - \gamma_{\text{opt}}^2} \end{aligned} \quad (5)$$

and

$$T_n = a + b \frac{1}{1 - \gamma_g^2} + c \frac{\gamma_g \cos(\theta_g - \theta_{\text{opt}})}{1 - \gamma_g^2}. \quad (6)$$

To comply with the physical meaning in the real transistor case, two constraints are added in this revised least squares fit. First, since γ_{opt} cannot be larger than one and $4T_0N$ is always smaller than T_{\min} , variables a and c must be negative, while b should be larger than zero [11]. Second, $(b + c)$ needs to be positive to again guarantee a smaller-than-one γ_{opt} . By contrast, these constraints will be hard to implement in the original four-variable situation [1].

Once $a, b,$ and c are derived and linearized, noise parameters of the transistor are ready to be obtained. In Fig. 8(a), both the minimum noise temperature T_{\min} and product $4T_0N$ have units of kelvin. The ratio of $4T_0N/T_{\min}$ is around 1.05 across the frequency range. Fig. 8(b) shows the optimum reflection coefficient Γ_{opt} that moves counterclockwise as frequency increases. Fig. 9 displays the measured and simulated noise temperatures in both matched and mismatched cases. Here, Fig. 9(a) corresponds to the matched case where the solid curve is the measured noise temperature, while the dashed curve is its simulated counterpart, which is reconstructed from the just-derived noise parameters. Fig. 9(b) shows the measured (solid curve) and simulated (dashed curve) noise temperatures in the mismatched case.

Comparisons with the model-based T_{\min} and $4T_0N$ can then be carried out, as displayed in Fig. 10. Here, Fig. 10(a) shows the minimum noise temperature where the solid curve is the measured result; the five dashed curves are with the transistor's drain temperature set from 1500 K (curve 1) to 3500 K (curve 5) with increment of 500 K between adjacent curves. Fig. 10(b) shows the corresponding $4T_0N$ curves. While a drain temperature of

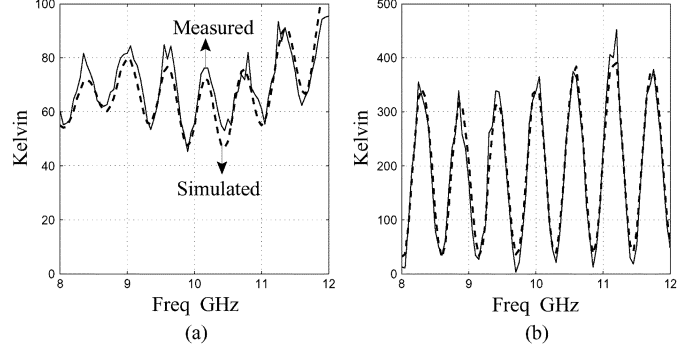


Fig. 9. 8–12-GHz matched and mismatched noise temperatures of the transistor. (a) Matched T_n . (b) Mismatched T_n .

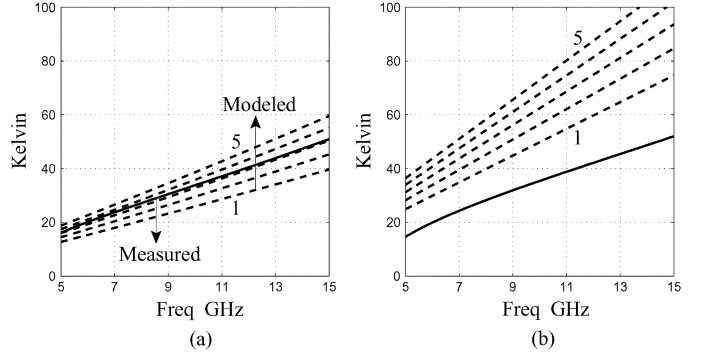


Fig. 10. Comparison of the measured and model-based T_{\min} and $4T_0N$ where the model is based on [1]. (a) T_{\min} . (b) $4T_0N$.

2500 K used in the model does have its T_{\min} most agreeing with the measured result, all the model-based $4T_0N$ values are, however, larger than the measured one and, thus, demand some explanations.

As has been indicated in [5], noise resistance is, among the four noise parameters, most susceptible to measurement errors. This can be observed through simulation where the mismatched T_n is deliberately shifted upwards: the resulting $4T_0N$ increases by roughly the same amount while only a fraction of that will be added on to T_{\min} . Possible measurement errors aside, one can attribute this $4T_0N$ discrepancy to the noise model employed where the intrinsic transistor's drain noise and gate noise are assumed to be uncorrelated. In [12] and [13], the derived noise resistance predicted by the zero-correlation model is noticeably lower across the frequency range than that measured by the tuner method, and agreement between measurement and model can only be achieved when nonzero noise correlation is allowed in the model. Thus, one might expect the $4T_0N$ curve of a revised model will be more in line with the measured one.

V. CONCLUSION

In this paper, the noise-parameter measurement of an ultra-sensitive transistor on-wafer at room temperature using the wide-band frequency-variation method has been carried out, and the measured results have been presented and investigated. In addition to this ultra-low-noise application, this approach is expected to be used, either alone or in combination with the tuner method, to facilitate noise measurements at even higher and broader frequency ranges.

ACKNOWLEDGMENT

Author R. Hu would like to thank Dr. S. Weinreb, G. Chattopadhyay, M. Edgar, D. Miller, F. Rice, J. Kooi, S. Lin, M. Yang, and Prof. J. Zmuidzinas, all of the California Institute of Technology, Pasadena, Prof. G. Rebeiz, The University of Michigan at Ann Arbor, MI, Dr. J. Ward, Jet Propulsion Laboratory (JPL), Pasadena, CA, Dr. F. Lo, National Radio Astronomy Observatory (NRAO), Charlottesville, VA, and Dr. P. Koch, M.P. Chen, and S. Y. Liu, all of Academia Sinica, Taiwan, R.O.C., for their support and encouragement. The authors thank Dr. D. Williams, National Institute of Standards and Technology (NIST), Boulder, CO, and the reviewers of this paper for their suggestions and comments.

REFERENCES

- [1] R. Hu and S. Weinreb, "A novel wide-band noise-parameter measurement method and its cryogenic application," *IEEE Trans. Microw. Theory Tech.*, vol. 52, no. 5, pp. 1498–1507, May 2004.
- [2] J. Gao, C. L. Law, H. Wang, S. Aditya, and G. Boeck, "A new method for pHEMT noise-parameter determination based on 50- Ω noise measurement system," *IEEE Trans. Microw. Theory Tech.*, vol. 51, no. 10, pp. 2079–2089, Oct. 2003.
- [3] C. E. McIntosh, R. D. Pollard, and R. E. Miles, "Novel MMIC source-impedance tuners for on-wafer microwave noise-parameter measurement," *IEEE Trans. Microw. Theory Tech.*, vol. 47, no. 2, pp. 125–131, Feb. 1999.
- [4] R. T. Weber, A. J. Slobodnik, and G. A. Roberts, "Determination of InP HEMT noise parameters and S -parameters to 60 GHz," *IEEE Trans. Microw. Theory Tech.*, vol. 43, no. 6, pp. 1216–1225, Jun. 1995.
- [5] M. W. Pospieszalski, "Modeling of noise parameters of MESFET's and MODFET's and their frequency and temperature dependence," *IEEE Trans. Microw. Theory Tech.*, vol. 37, no. 9, pp. 1340–1350, Sep. 1989.
- [6] N. Niklas, A. Mellberg, I. Angelov, M. E. Barsky, S. Bui, E. Choumas, R. W. Grundbacher, E. L. Kollberg, R. Lai, N. Rorsman, P. Starski, J. Stenarson, D. C. Streit, and H. Zirath, "Cryogenic wide-band ultra-low-noise IF amplifiers operating at ultra-low dc power," *IEEE Trans. Microw. Theory Tech.*, vol. 51, no. 6, pp. 1705–1711, Jun. 2003.
- [7] R. Hu, "An 8–20-GHz wide-band LNA design and the analysis of its input matching mechanism," *IEEE Microw. Wireless Compon. Lett.*, vol. 14, no. 11, pp. 528–530, Nov. 2004.
- [8] L. Escotte, R. Plana, and J. Graffeuil, "Evaluation of noise parameter extraction methods," *IEEE Trans. Microw. Theory Tech.*, vol. 41, no. 3, pp. 382–387, Mar. 1993.
- [9] R. O. Schmidt, "Multiple emitter location and signal parameter estimation," in *Proc. RADC Spectral Estimation Workshop*, Rome, NY, 1979, pp. 243–258.
- [10] R. H. Roy, A. Paulraj, and T. Kailath, "ESPRIT—A subspace rotational approach to estimation of parameters of cisoids in noise," *IEEE Trans. Acoust., Speech, Signal Process.*, vol. ASSP-34, pp. 1340–1342, 1986.
- [11] M. W. Pospieszalski, "On the measurement of noise parameters of microwave two-ports," *IEEE Trans. Microw. Theory Tech.*, vol. MTT-34, no. 4, pp. 456–458, Apr. 1986.
- [12] J. H. Han and K. Lee, "A new extraction method for noise sources and correlation coefficient in MESFET," *IEEE Trans. Microw. Theory Tech.*, vol. 44, no. 3, pp. 487–490, Mar. 1996.
- [13] J. Stenarson, M. Garcia, I. Angelov, and H. Zirath, "A general parameter-extraction method for transistor noise models," *IEEE Trans. Microw. Theory Tech.*, vol. 47, no. 12, pp. 2358–2363, Dec. 1999.



Robert (Shu-I) Hu received the B.S.E.E. degree from National Taiwan University, Taipei, Taiwan, R.O.C., in 1990, and the Ph.D. degree from The University of Michigan at Ann Arbor, in 2003.

From 1996 to 1999, he was with Academia Sinica, Taipei, Taiwan, R.O.C., where he was involved with millimeter-wave receivers. In 1999 and 2003, he was with the California Institute of Technology, Pasadena, where he was involved with millimeter-wave wide-band receivers. He is currently with National Chiao-Tung University,

Taiwan, R.O.C. His research interests include microwave and millimeter-wave electronics.



Tzu-Hsien Sang received the B.S.E.E. degree from National Taiwan University, Taipei, Taiwan, R.O.C., in 1990, and the Ph.D. degree from The University of Michigan at Ann Arbor, in 1999.

He is currently an Assistant Professor with National Chiao-Tung University (NCTU), Taiwan, R.O.C. Prior to joining NCTU in 2003, he was with the start-up company Excess Bandwidth, Sunnyvale, CA, where he was involved with the physical layer design for broad-band technologies, mainly xDSL.

His research interests include signal-processing techniques for communications, time-frequency analysis, and noise modeling for high-frequency solid-state devices.